Robustness and Coherence of a Three-Protein Circadian Oscillator: Landscape and Flux Perspectives

Jin Wang,[†‡*] Li Xu,[†§] and Erkang Wang[†*]
[†]State Key Laboratory of Electroanalytical Chemistry, Changchun Institute of Applied Chemistry, Chinese Academy of Sciences, Changchun, Jilin, China; [‡]Department of Chemistry & Department of Physics, State University of New York at Stony Brook, Stony Brook, New York; and [§]Graduate School of the Chinese Academy of Sciences, Beijing, China

ABSTRACT Three-protein circadian oscillations in cyanobacteria sustain for weeks. To understand how cellular oscillations function robustly in stochastic fluctuating environments, we used a stochastic model to uncover two natures of circadian oscillation: the potential landscape related to steady-state probability distribution of protein concentrations; and the corresponding flux related to speed of concentration changes which drive the oscillations. The barrier height of escaping from the oscillation attractor on the landscape provides a quantitative measure of the robustness and coherence for oscillations against intrinsic and external fluctuations. The difference between the locations of the zero total driving force and the extremal of the potential provides a possible experimental probe and quantification of the force from curl flux. These results, correlated with experiments, can help in the design of robust oscillatory networks.

INTRODUCTION

Biological rhythms widely exist in living organisms, such as membrane potential oscillations, cardiac rhythms, calcium oscillations, glycolytic oscillations, cell cycles, and circadian clocks. In the cell, molecules are nearly finite in number (typically approximately several hundreds). Therefore, the intrinsic statistical fluctuations, usually not encountered in the bulk due to the large number averaging, can be significant. On the other hand, the fluctuations from highly dynamical and inhomogeneous environments of the cell interior provide the source of the external noise (1–8). Therefore, it is important to investigate how the rhythms robustly function against the stochastic fluctuations.

The underlying causes of the cellular rhythmic behavior have been explored by experimental and theoretical approaches (9–18). For example, oscillations have been found to be robust and sustain for weeks for the circadian clock in cyanobacteria (13–18). Circadian rhythms involve an intracellular timing mechanism that widely exists in living organisms with a period of ~24 h, adapting to the day/night alterations of the earth in fluctuating environments. In *Neurospora*, *Arabidopsis*, *Drosophila*, and mammals, transcription-translation-derived oscillations originating from negative feedback regulation of clock genes have been modeled at the molecular level (10–12).

Recently, researchers have uncovered the existence of a circadian clock, which has no transcription-translation feedback loop, in the cyanobacteria system (13–18). Three proteins, KaiA, KaiB, and KaiC, play important roles in the circadian rhythms. The oscillator can be reconstituted and observed by incubating three purified proteins and the adenosine triphosphate (ATP) in vitro. This provides a good opportunity for studying the underlying circadian mechanisms with more controls (13–17). Kai proteins accumulate, synthesize, degrade, form complexes, and phosphorylate in the cyanobacterial cell. KaiC is an enzyme with autokinase and autophosphatase activities, and is hexameric, with two KaiC phosphorylation sites, i.e., at the residues Ser^{431} and Thr^{432}. The circadian rhythm (13–17) diminishes completely when those two residues are substituted with alanine. The dimeric KaiA enhances the autophosphatase of KaiC, while KaiB reduces the activity of KaiA on KaiC. In Fig. 1, we show a cyclic reaction diagram depicting the protein-protein interactions and phosphorylation-dephosphorylation events between the Kai proteins. In the oscillation, KaiA actively and repeatedly associated with the KaiC hexamer to activate KaiC phosphorylation in the phosphorylation phase. When the KaiC proteins maximally phosphorylate, KaiB binds on either KaiC or the KaiA-KaiC complex and inactivates KaiA to start the dephosphorylation phase. Therefore, the process switches from the phosphorylation phase to the dephosphorylation phase. As the KaiC decreases its phosphorylation, KaiB and KaiA dissociate from KaiC and reactivate KaiA, and then the cycle returns to the KaiC phosphorylation phase. This completes an oscillation cycle.

In modern systems biology, studying oscillation behavior in an integrated and coherent way is crucial for the understanding of how the rhythm functions, both biologically and robustly. The biological clock dynamics is often described, theoretically, by deterministic or stochastic chemical reaction networks (10–12,18). Complex nonlinear phenomena can emerge from these studies, such as bifurcations and chaos. With slightly different initial conditions, the system characterized by the trajectories of the protein concentrations can behave in drastically differential ways. The resulting dynamics can lead to periodic oscillations (i.e., limit cycles). Robustness is typically only analyzed locally around the

Submitted March 3, 2009, and accepted for publication September 10, 2009.

*Correspondence: jin.wang.1@stonybrook.edu or ekwang@ciac.jl.cn

Editor: Kathleen B. Hall.

0006-3495/09/12/3038/9 $2.00

doi: 10.1016/j.bpj.2009.09.021

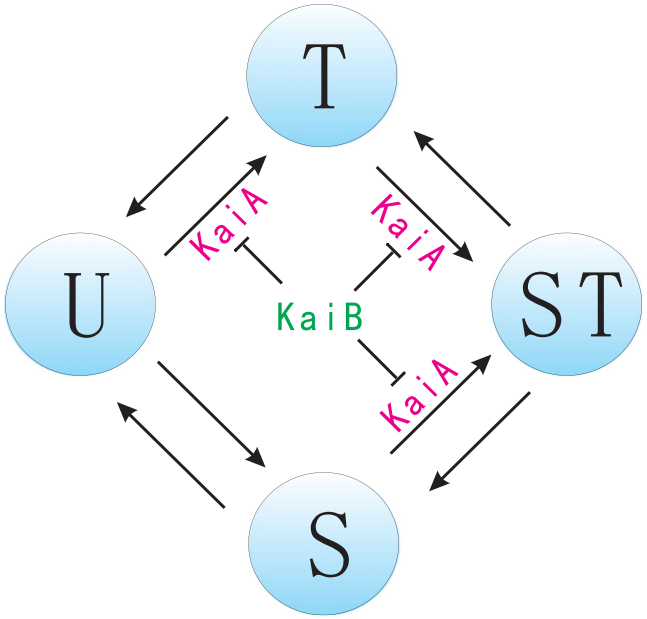

FIGURE 1 The three-Kai oscillator when ATP is provided in excess.

fixed points or limit cycles. Global stability is still hard to see using current methods.

Here, instead of focusing on deterministic or stochastic trajectories that are local in nature, we developed a global approach to robustness of circadian oscillation in cyanobacteria by directly exploring the probabilistic distribution in the whole protein concentration space (therefore global) for oscillations with a stochastic model. The current approach (19–29) enables us to borrow some fruitful analysis from energy landscape theory of protein folding (30), where quasi-equilibrium is often assumed, whereas here we emphasize the nonequilibrium properties.

Therefore, going beyond the approach with the averaged deterministic network of chemical rate equations, we need to develop a probabilistic description to model globally the probabilistic nature of the corresponding cellular process taking the intrinsic and external fluctuations into account. This can be realized by constructing a master equation for the intrinsic fluctuations or the diffusion equation for external fluctuations of the time-dependent evolution probability instead of average concentration for the corresponding deterministic chemical reaction network equations (4,31–35). Even for the intrinsic fluctuations, we can simplify the master equation into a Fokker-Planck, diffusionlike equation in the weak noise limit representing a typical kinetic Markovian behavior (36). Therefore, we can use the diffusion equation to approximate the system probabilistically under the influence of either internal or external fluctuations.

By solving the corresponding Fokker-Planck diffusion equation, we can obtain the probability distribution in protein concentrations evolving in time. We can also uncover the long-time steady-state probability of this chemical reaction network. Analogous to the equilibrium system in which the global thermodynamic properties can be explored by knowing the inherent interaction potentials, we will study the global stability by exploring the underlying potential landscape for the circadian oscillatory nonequilibrium protein network. The generalized potential can be shown to be closely associated with the steady-state probability of the nonequilibrium network in general, and has been applied to a few systems (19–32,37,38). Once the network problem is formulated in terms of the generalized potential function or potential landscape, the issue of the global stability or robustness is much easier to address (24,26–29). We notice that although the individual averaged deterministic trajectories of a nonlinear chemical reaction system might be very chaotic and complex, the corresponding statistical probabilistic distributions or underlying landscapes, which are dictated by the linear evolution equations (master equations or diffusion equations), are usually quite ordered and can often be characterized globally.

The adaptive landscape idea was first introduced into biology by Fisher (39), Wright (40), Delbruck (41), and Waddington (42). The landscape ideas were further pushed forward by Frauenfelder et al. (43) on protein dynamics and then Wolynes et al. (30) on protein folding and interactions (44). All these ideas were based on equilibrium approach by knowing the potentials a priori. For our nonequilibrium system, potential landscape is not known at the beginning and needs to be uncovered. In fact, it is the purpose of this article, to study the global robustness of oscillation against fluctuations in the cell, directly from the properties of the potential landscape, linked to the steady-state probability of the network. This provides a basis for exploring the global and physical mechanism of biochemical oscillation.

METHODS AND MATERIALS

We decide to explore the global probabilistic nature of an established model based on known biological and biochemical features of KaiC oscillation in vitro, which does not involve a transcription or translation process when ATP is provided in excess (13–18). It is shown that biochemical interactions among KaiA, KaiB, and KaiC proteins drive the circadian oscillations of KaiC phosphorylation both in vitro and in vivo, although a regulatory mechanism of the KaiC phosphorylation process remains unclear (13–18). We quantify the four possible time-dependent phosphorylation states: unphosphorylated (U-KaiC), phosphorylated only on S431 (S-KaiC), phosphorylated only on T432 (T-KaiC), and phosphorylated on both S431 and T432 (ST-KaiC).

The dynamical variables of our model are T (concentration of T-KaiC), D (concentration of the doubly phosphorylated form ST-KaiC), and S (concentration of S-KaiC). U (concentration of U-KaiC) follows from conservation of total KaiC concentration ([KaiC]). The kinetics of the interconversions between phosphoforms are first-order, but with the rates depending on S.

A deterministic mathematical model of this protein clock constrained by experimental data has been proposed recently (18). For the protein network, based on Michaelis-Menten enzyme kinetic equations, one can derive a set of differential equations that describe the variation rate of each component's concentration in the network. We have two independent simplified equations (18),

$$\frac{dT}{dt} = k_{UT}(S)U + k_{DT}(S)D - k_{TU}(S)T - k_{TD}(S)T, \quad (1)$$
$$= F_1(T,D,S)$$

$$\frac{dD}{dt} = k_{TD}(S)T + k_{SD}(S)S - k_{DT}(S)D - k_{DS}(S)D, \quad (2)$$
$$= F_2(T,D,S)$$

$$\frac{dS}{dt} = k_{US}(S)U + k_{DS}(S)D - k_{SU}(S)S - k_{SD}(S)S, \quad (3)$$
$$= F_3(T,D,S)$$

$$A = \max\{0, [Kai\,A] - 2mS\}, \quad (4)$$

$$k_{XY}(S) = k^0_{XY} + \frac{k^A_{XY}A(S)}{K_{1/2} + A(S)}, \quad (5)$$

where A is the concentration of active KaiA monomers, and [KaiA]is the total concentration of KaiA monomers. A is defined as [KaiA] minus a multiple 2m of the concentration of S (which inhibits KaiA via KaiB). We use the simplest choice $m = 1$, corresponding to the inactivation of one KaiA dimer by one S-KaiC monomer. The value k_{XY} shows the rate constant for the transition from state X to state Y. The value k^0_{XY} represents the rate in the absence of KaiA, and k^A_{XY} represents the maximum influence of KaiA on that rate. If KaiA promotes the transition, then $k^A_{XY} > 0$ means that KaiA promotes the transition, whereas $k^A_{XY} < 0$ means that KaiA inhibits the transition. $K_{1/2}$ is the total concentration of KaiA causing a half-maximal effect on KaiC's autophosphorylation rates.

As mentioned, the statistical fluctuations can be important from both internal and external sources (1–8), and in general, cannot be ignored. To study the global robustness and function of circadian clock probabilistically, we now formulate the Fokker-Planck diffusion equation for the time evolution of the probability distributions of protein concentrations for T, D, and S,

$$\frac{\partial P(T,D,S,t)}{\partial t} = -\frac{\partial}{\partial T}[F_1(T,D,S)P] - \frac{\partial}{\partial D}[F_2(T,D,S)P] - \frac{\partial}{\partial S}[F_3(T,D,S)P] + D_c\left(\frac{\partial^2 P}{\partial T^2}\right) + D_c\left(\frac{\partial^2 P}{\partial D^2}\right) + D_c\left(\frac{\partial^2 P}{\partial S^2}\right). \quad (6)$$

Where D_c is the diffusion coefficient tensor(or matrix), we use a uniform diagonal matrix for simplicity.

We set vector $\mathbf{x} = (T, D, S)$. We can rewrite the diffusion equation as $\frac{\partial P}{\partial t} = \nabla \cdot J(\mathbf{x}, t)$ and define the flux vector of the system as

$$J(\mathbf{x},t) = \mathbf{F}P - \mathbf{D}_c \cdot \frac{\partial}{\partial \mathbf{x}}P, \quad (7)$$

or in the component notation,

$$J_1(T,D,S,t) = F_1(T,D,S)P - D_c\frac{\partial}{\partial T}P,$$

$$J_2(T,D,S,t) = F_2(T,D,S)P - D_c\frac{\partial}{\partial D}P,$$

and

$$J_3(T,D,S,t) = F_3(T,D,S)P - D_c\frac{\partial}{\partial D}P,$$

where $J(\mathbf{x}, t)$ is the probability flux vector in the three-dimensional protein concentration space. In steady state, the J is the divergent free flux with $\nabla \cdot J(\mathbf{x}, t) = 0$. It is obvious that in the steady state the divergence of J must vanish (since $\partial P/\partial t = 0$). One cannot conclude, however, that J itself must vanish. Only in the equilibrium situation where the systems satisfying the detailed balance, $J = 0$. For the nonequilibrium system in general, the steady state contains a circulating flow with nonzero curl. This is because the divergent flux has neither source to come from nor sinks at which to end. It can only go around. We notice from the definition that

$$\mathbf{J}_{ss} = \mathbf{F}P_{ss} - \mathbf{D}_c \cdot \frac{\partial}{\partial \mathbf{x}}P_{ss}.$$

Therefore,

$$\mathbf{F} = \mathbf{D}_c \cdot \frac{\partial}{\partial \mathbf{x}}P_{ss}/P_{ss} + \mathbf{J}_{ss}/P_{ss} = -\mathbf{D}_c \cdot \frac{\partial}{\partial \mathbf{x}}(-\ln P_{ss}) + \mathbf{J}_{ss}/P_{ss} = -\mathbf{D}_c \cdot \frac{\partial}{\partial \mathbf{x}}U + \mathbf{J}_{ss}/P_{ss}\Big).$$

P_{ss} stands for steady-state probability. Although $\mathbf{F}$ in general cannot be represented as a potential gradient, the driving force for the dynamics can be decomposed to two terms for nonequilibrium network systems. One is associated with the gradient of a potential closely linked to the steady-state probability (the nonequilibrium potential U can be defined as $U = -\ln P_{ss}$), and the other is associated with a divergent free flux curling around (29).

Once we have the steady-state probability we can study the underlying properties of the potential (or potential landscape) by the relation: $U(\mathbf{x}) = -\ln P(\mathbf{x})$. This relationship for our nonequilibrium systems (no detailed balance or equivalently F is not a gradient of a potential) is motivated in analogy with the equilibrium systems when F can be represented as a gradient of a potential and the steady-state probability is exponentially linked with the potential. Unlike in the equilibrium systems where only the steady-state probability is needed to characterize the global properties of the whole system, in the nonequilibrium systems, both the underlying potential landscape and the associated flux are essential in characterizing the global steady-state properties as well as the dynamics of the protein network.

RESULTS AND DISCUSSIONS

Landscape of the circadian clock

We fix all the kinetic parameters except the total concentration of KaiC, KaiA, and the binding constant K_d of KaiA-KaiC interaction. The other parameter values are in Table S1 of the Supporting Material. When we choose a set of specific parameters $KaiC = 3.4\ \mu$m, $Kai\,A = 1.3\ \mu$m, and $K_{1/2} = 0.43\ \mu$m, the fixed point is unstable (18). The limit cycle emerges.

We solve the Fokker-Planck diffusion equation for the probability distribution of the three proteins T, D, and S, using both the reflecting boundary condition $J = 0$ and the absorbing boundary condition. The results are similar. We choose the reflecting boundary condition in this article. With certain initial conditions (both homogeneous and inhomogeneous),we obtain the steady probability distribution solution P using finite difference method at the long time limit. Then, we can use $U(\mathbf{x}) = -\ln P(\mathbf{x})$ to obtain the generalized potential function as well as the corresponding curl flux of the nonequilibrium circadian clock.

To see the results clearly, we can integrate the three-dimensional probability $P(T,D,S,t \to \infty)$ to reduce the dimensionality. We can use the following integration formula:

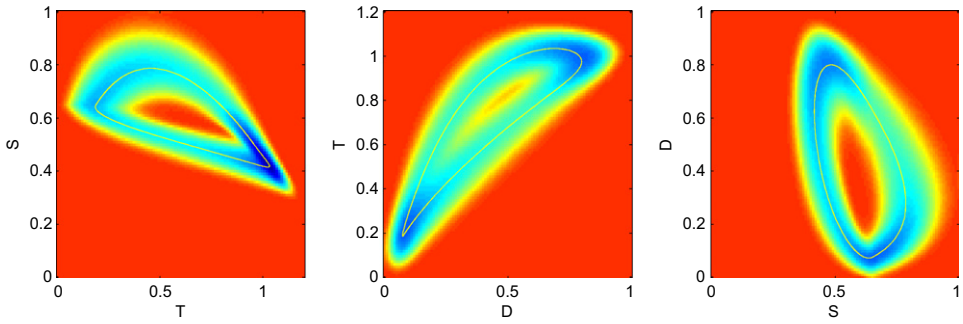

FIGURE 2 The integrated results for the three-dimensional system.

$$P_{\mathrm{S}}(T,D,t\to\infty) = \int_{\mathrm{S}} P(T,D,S,,t\to\infty)\mathrm{dS}$$
$$P_{\mathrm{D}}(T,S,t\to\infty) = \int_{\mathrm{D}} P(T,D,S,,t\to\infty)\mathrm{dD}\,. \quad (8)$$
$$P_{\mathrm{T}}(D,S,t\to\infty) = \int_{\mathrm{T}} P(T,D,S,,t\to\infty)\mathrm{dT}$$

The integrated results are shown in color contour plots of potential landscape versus corresponding protein concentrations in Fig. 2. The yellow solid lines represent the deterministic oscillatory orbit of the circadian clock. The blue color represents the low potential and red color represents the high potential. We can see the potential landscape has an irregular inhomogeneous ring or Mexican-hat-like shape, with lower potential along the oscillation ring and higher potential outside of the oscillation ring.

Fig. 3 *A* shows the potential landscape U in three protein concentration dimensions (U, S, and T), with a distinct irregular and inhomogeneous closed-doughnut-like shape. To see clearly, we only plot the three-dimensional $U \leq 17.3$, while $U > 17.3$ is transparent. The closed doughnut is around the deterministic solution that represents the lower potential and corresponding higher probability along the oscillation trajectories. The potential is higher and the probability is lower outside the doughnut. So the system is attracted to the closed doughnut. We found that the potential landscape inhomogeneously distributes along the oscillation ring. The potential is lower for longer stay-time at each state. The stay time at each state is due to the speed passing through each state of the averaged deterministic oscillation. Therefore, the potential landscape and the steady-state probability along the oscillation are not uniform due to the inhomogeneity of the time spent and the passing speed on each state. We also observe the doughnut of the potential landscape is thicker, and the values of the potential landscape along the limit cycle became smaller than the inside and the outside of the limit cycle, upon increase of the diffusion coefficient D_{c}, which represents the strength of the fluctuations. A further increase in the fluctuations will eventually obliterate circadian rhythmicity. It implies the system has more freedom to go everywhere under large fluctuating environments. This is because the attraction of the limit cycle became weaker and the time spent on the limit cycle became shorter. The system experiences a transition from a clear oscillation under small fluctuations to an obliterated one under large fluctuations. These results show the oscillation is more robust and attractive under fewer fluctuations.

The divergence of the flux is equal to zero at steady state. In equilibrium system, the flux $\mathbf{J} = 0$ for detailed balance. However, in the nonequilibrium system, the flux is a curl field ($J = \nabla \times A$, where A is a vector field). Fig. 3 *B* shows the probability flux on the closed ring landscape of the limit cycle. To demonstrate the origin of the curl flux J, we should study the chemical rate force F. The force from negative gradient of the landscape is written as $-\nabla U(\mathbf{x})$. We define the residual force as

$$\mathbf{F}'(\mathbf{x}) = \mathbf{F}(\mathbf{x}) - (-D_{\mathrm{c}}\nabla U(\mathbf{x})) = \mathbf{F}(\mathbf{x}) + D_{\mathrm{c}}\nabla U(\mathbf{x}). \quad (9)$$

Therefore, the real force $\mathbf{F}(\mathbf{x})$ is the summation of the gradient force and the residual force. The residual force is the driving force for the curl field of the probability flux. The potential landscape attracts the system to the closed ring and the residual force drives the oscillation along the ring (by keeping the probability flux moving along the ring). We can see that the residue force plays a more important role along the closed ring. Therefore, both the gradient force from the potential

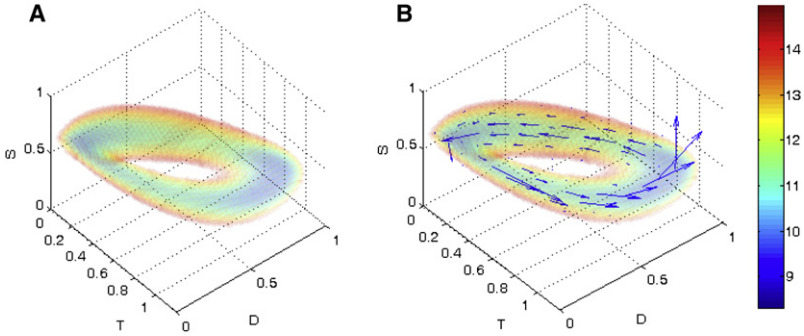

FIGURE 3 The landscape and flux in the three dimensions T, D, and S of the circadian clock.

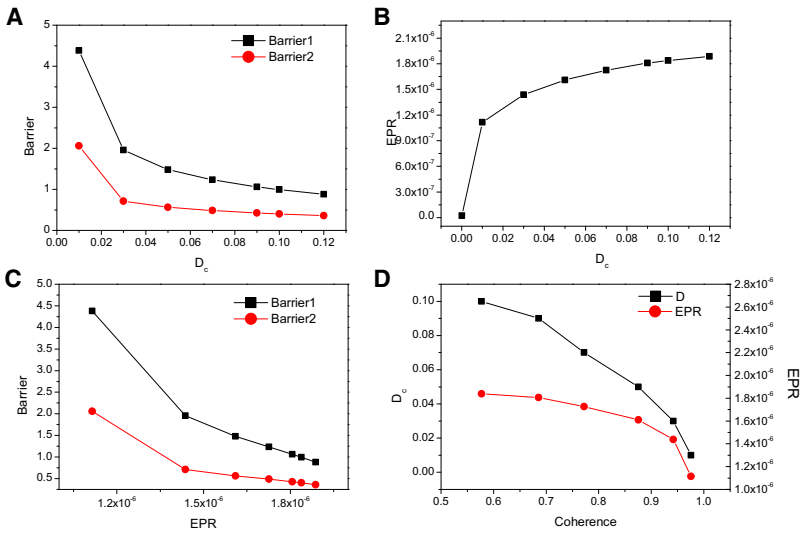

FIGURE 4 (*A*) The barrier height $Barrier1 = U_{fix} - U_{min}$ and $Barrier2 = U_{fix} - U_{max}$ versus diffusion coefficient D_c. (*B*) The diffusion coefficient D_c versus the entropy production rate. (*C*) The barrier height $Barrier1 = U_{fix} - U_{min}$ and $Barrier2 = U_{fix} - U_{max}$ versus the entropy production rate. (*D*) The coherence versus the diffusion coefficient D_c and the entropy production rate.

landscape and the residual force from the curl flux are the characteristics for a nonequilibrium system.

It is very important to note that the fixed points in the deterministic dynamical systems are defined as where the total force F is equal to zero. However, as we have seen, the total force can be decomposed into the gradient of a potential and a residual force from curl flux. Because the residual force is, in general, not equal to zero for the nonequilibrium systems, the locations where the gradient potential force is equal to zero are not necessarily exactly the same as those in which the total force F is equal to zero (45,46).

This is quite interesting in the following three senses:

1. The potential is coming directly from the probability distribution of the observables, and the deterministic equation of motion is often the first-order moment (or average) equations of motion of the observables.
2. The discrepancy of the locations reflects the fact that the peak of the distribution may not be the same as the average of the observables.
3. The shift of the location is also a reflection of the presence of the residual force from the curl flux. When the residual force is not equal to zero, the gradient force and total force are not equal and the zero force (gradient and total) location in general will be different.

This suggests an experimental way to probe the effects of the curl flux force by looking at the probability distribution of the observables to find out the location of the peaks as well as the averages. The difference between them may give us some hints and quantitative information on the existence of the residual force from the curl flux.

Barrier height, stability, coherence, and dissipation

We can explore the global stability and the robustness of the circadian clock when we obtain the potential landscape. The barrier height represents the degree of difficulty for the system escaping from the oscillation attractor to outside. Therefore the barrier height is a direct quantitative measure of the stability. Fig. 4 *A* shows the barrier height versus the diffusion coefficient D_c. *Barrier*1 is equal to U_{fix} minus U_{max}, and *Barrier*2 is equal to U_{fix} minus U_{min}, where U_{fix} is the potential energy local maximum inside the limit cycle; U_{max} is the potential maximum along the limit cycle; and U_{min} is the potential minimum along the limit cycle. We can see the barrier height become higher when the fluctuations decrease. It becomes harder for the system to go from the doughnut of attraction to the outside; this results in fewer fluctuations. In this case, the circadian clock is more stable and robust.

The circadian clock is a nonequilibrium, open system that can exchange information and energies with the outside. In the nonequilibrium steady state, the system will dissipate energy and entropy. The dissipation is determined by both the landscape and the flux. This is in analogy to electrical circuit where the heat loss is determined by the combined electric current and potential. Here for nonequilibrium network, the potential landscape and flux play the roles of electric potential and current for the electric circuit. In the steady state, the entropy production rate equals to heat dissipation ((47), and see details in the Supporting Material). In Fig. 4 *B*, we can see the dissipation (entropy production rate) decrease as the diffusion coefficient, characterizing the fluctuations, decreases. It shows the robust oscillation with fewer fluctuations dissipates less energy and is more stable. In Fig. 4 *C*, we also see that less dissipation leads to higher barrier heights escaping from the oscillation cycle and therefore, a more stable network. Thus, minimization of the dissipation cost might serve as a design principle for evolution of the network, because the entropy production is a global characterization of the circadian network. The dissipation characterized by the entropy production is related intimately to the robustness of the network.

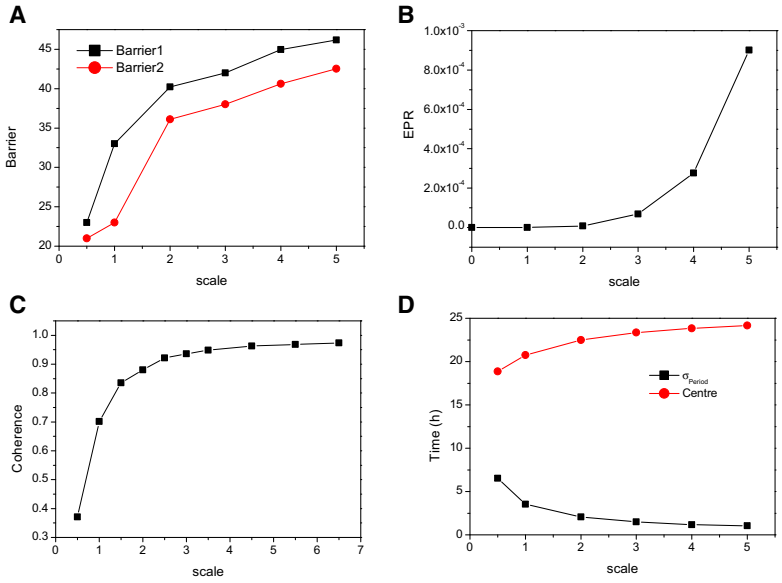

FIGURE 5 (*A*) The barrier height versus the scale. (*B*) The entropy production rate versus the scale. (*C*) The coherence versus the scale. (*D*) The standard deviation of period σ_{Period} and the mean of the period versus the scale.

We have explored the phase coherence ξ, which can measure the degree of periodicity of the time evolution of a given protein concentration variable to address the robustness of the oscillation ((48), and see details in Supporting Material). The value of ξ becomes larger when the fluctuation is less, since the trajectories are more periodic (ossilating more regularly) in the evolution. Fig. 4 *D* shows ξ-values became lower as the diffusion coefficient became larger. It implies that the coherence of the oscillation can be destroyed by the fluctuations. With less fluctuation, and a more coherent system, the oscillation is more robust and stable. In addition, a less-dissipated network tends to preserve the coherence of the oscillations. Therefore, more coherent oscillations require a more robust and less-dissipated network.

Stability, dissipation, and period under scale and equilibrium-constant changes

It is reported that increasing the concentration of all three Kai proteins, up to at least fivefold above the standard concentrations, has no effect on the oscillation of KaiC phosphorylation in the in vitro reaction (45). Rust et al. (18) confirm that oscillations occur between 0.5- and fourfold the Kai protein concentration. However, by monitoring the reaction for longer than Kageyama et al. (45), they find that there is an increase in period as the concentration is increased ~0.5- to fourfold (18). Therefore, we solve the Fokker-Planck probabilistic diffusion equations for the system, because every protein concentration is increased 0.5- to fourfold using the modified model. We choose the bimolecular association of KaiA and KaiC as a preequilibrium described by a binding constant $K_d = 1$. We can see that the barrier height increases when the scale increases in Fig. 5 *A*. Therefore, having more proteins available tends to better stabilize the system. In Fig. 5 *B*, it shows the entropy production rate versus the scale. The more proteins, the higher the entropy production rate. We can also see that the coherence increases when the scale increases in Fig. 5 *C*. It implies the noise has less influence with more proteins. In Fig. 5 *D*, it shows the standard deviation and the mean of the period of ossilation versus the scale. It implies the period increases and dispersion of period decreases gradually as the concentration is increased from ~0.5- to fourfold. The fluctuations during this period become fewer, with the presence of more proteins. This is consistent with the experimental results obtained by Kageyama et al. (45) and modeling results from Rust et al. (18), and provides understanding from a landscape perspective. More proteins lead to higher barrier height of the underlying network landscape topography. This then leads to a more coherent and stable oscillation. It further leads to a longer period and less dispersion of the oscillations.

The original model does not account for the near independence of period and amplitude on Kai protein concentrations (18). However, the value $K_{1/2}$ of the level of active KaiA is not independent of the concentrations. In a modified model (see Supporting Material for details), Rust et al. reported bimolecular association of KaiA and KaiC as a preequilibrium described by a binding constant K_d (18). They showed that the period increases as the K_d increases when the scale is >1, and the period decreases as the K_d increases when the scale is <1.

We solve the Fokker-Planck probabilistic diffusion equation for *scale* $= 2$. In Fig. 6, we find that the barrier height decreases as the K_d increases (*A*), the entropy production rate increases as the K_d increases (*B*), the coherence is nearly unchanged as the K_d increases (*C*), and the period increases slightly as the K_d increases (*D*). This is consistent with what Rust et al. observed (18). For large scales, the protein concentrations are large, and there will be fewer intrinsic fluctuations to influence the stability of the systems. As K_d

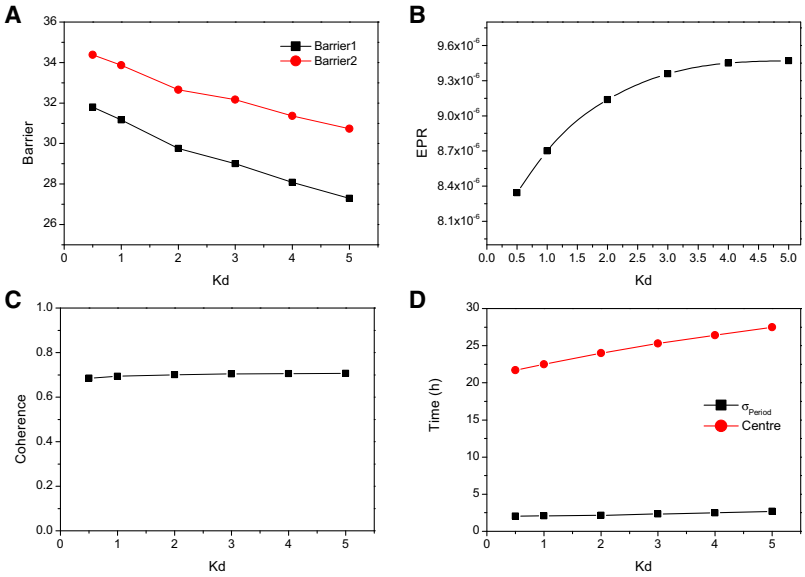

FIGURE 6 *Scale* = 2. (*A*) The barrier height versus K_d. (*B*) The entropy production rate versus K_d. (*C*) The coherence versus K_d. (*D*) The standard deviation of period σ_{Period} and the mean of the period versus K_d.

increases, the fraction of time that active *KaiA* must be bound to a given *KaiC* monomer, to significantly promote its phosphorylation (represented by $K_{1/2}$), decreases. However, the phosphorylation is crucial for the completion of the oscillation. Decreasing of the phosphorylation leads to a more fragile landscape—i.e., having a lower barrier height makes it easier to go from one state to another, therefore making it less stable. In addition, a less stable system costs more to maintain and takes longer to complete the oscillation period.

Key rate parameters for stability and robustness

To explore the effects of the rate parameters on the stability and robustness, we explore which reactions are important and further, which protein elements are crucial for maintaining the robustness. Fig. 7 shows the effects of the rate parameters on the robustness. The eight parameters increase 10%, and decrease 10%. The bars show the barrier height change with different parameters. We can choose rates k^A_{SD} and k^A_{DT} for they are the most crucial reactions. The value q is the percent for increasing or decreasing the rate constants.

In Fig. 8, we show that the barrier height decreases and the entropy production rate increases as the parameter q increases for rate k^A_{SD}, and the barrier height increases and the entropy production rate decreases as the parameter q increases for rate k^A_{DT}. Since barrier height is a quantitative measure of how difficult it is to go from one part of the state space to the other, the higher the barrier, the harder it is to communicate from one place to another. The system is more stable, as the states are not easily changed from one to the other. It implies the system becomes more stable and robust when k^A_{SD} decreases or k^A_{DT} increases.

CONCLUSIONS

We uncovered two distinct factors essential for characterizing the global probabilistic dynamics for circadian oscillations in cyanobacteria (13–18): the underlying potential landscape directly (logarithmically) related to the steady-state probability distribution; and the corresponding flux related to the speed of the protein concentration changes. We found that the underlying potential landscape for the oscillation has a distinct closed-ring-valley shape when the fluctuations are small. This global landscape structure leads to attractions of the system to the ring-valley. On the ring, we found that the nonequilibrium flux is the driving force for oscillations. Therefore, both structured landscape and flux are needed to guarantee a global robust oscillation.

The barrier height separating the oscillation ring, and other areas derived from the landscape topography correlated with the escaping time from the limit cycle attractor, provide a quantitative measure of the network's robustness.

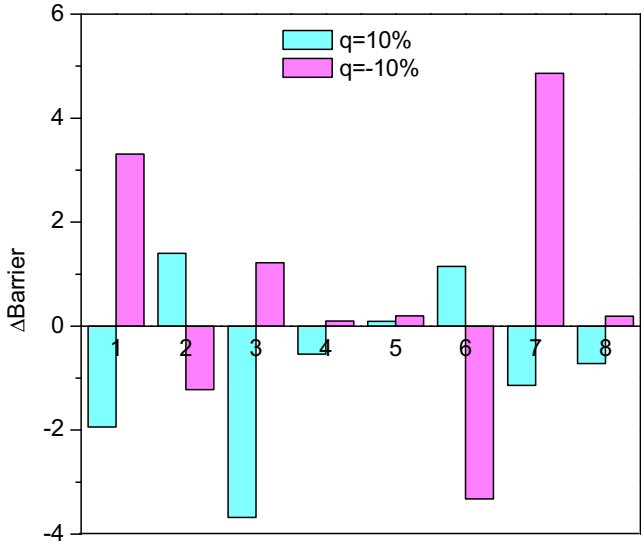

FIGURE 7 The change of barrier height versus q for eight rate constants: 1, k^A_{SD}; 2, k^A_{UT}; 3, k^A_{TD}; 4, k^A_{US}; 5, k^A_{TU}; 6, k^A_{DT}; 7:k^A_{DS}; and 8, k^A_{SU}.

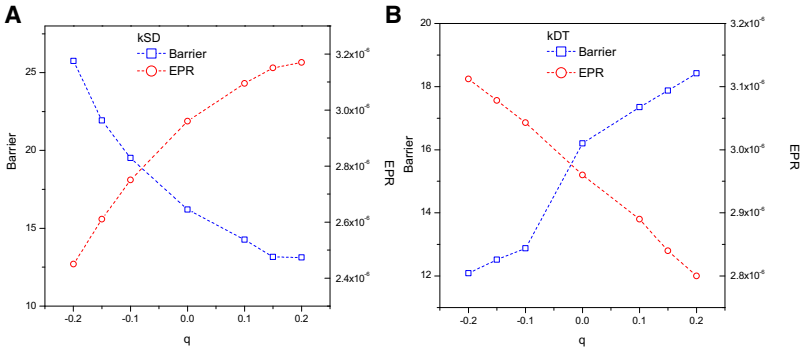

FIGURE 8 (*A*) The barrier height and entropy production rate versus q for k_{SD}^{A}. (*B*) The barrier height and entropy production rate versus q for k_{DT}^{A}.

The landscape becomes shallower and the closed-ring-valley shape structure becomes weaker (lower barrier height) with larger fluctuations. We observe that the period and the amplitude of the oscillations are more dispersed and oscillations become less coherent when the fluctuations increase.

We observe the global dissipation in terms of the entropy production, which increases in the whole system as the fluctuations increase. Lower entropy production correlates with high barrier height and therefore, a more stable and robust system. Minimization of dissipation cost might provide a guiding principle for network design.

When the fluctuations become very large, the landscape is flattened-out and coherence of the oscillations is destroyed. Robustness decreases. When the fluctuations are small, changing such inherent parameters of the system as chemical rates, equilibrium constants, and concentrations can lead to different robust behaviors.

We can also see that the coherence increases when the scale increases since the intrinsic noise is less for more proteins. The more proteins have more entropy production rate. The standard deviation of period of ossilation decreases and the mean of the period increase as the concentration is increased on the scale from ~0.5- to fourfold.

By exploring the sensitivity of barrier height on the parameters of the system, we find concentrations of Kai and the associated binding constants k_{SD}^{A} and k_{DT}^{A} important for robust oscillations. This provides a basis for reengineering and design.

We have used a stochastic model to uncover the underlying landscape of circadian clock oscillation. We found barrier heights to be a quantitative measure for robustness. These results correlated with others found in the literature (13–18), and we propose that they can aid in the design of more robust networks, in which the wiring can be reengineered against fluctuations.

A very simple two-dimensional limit cycle model was studied recently in Zhu et al. (49). A solution of constant radii and constant speed oscillation emerges. The limit cycle dynamics is uniform along the oscillation ring and isotropic along the radial direction. The authors (49) attempted to study, systematically, the global dynamics via adaptive landscape. In this work, we considered a general limit cycle dynamics in three dimensions where the oscillation is at nonuniform speed and is proceeding along an irregular closed tube. The resulting landscape is an irregular donut with nonuniform landscape and flux on the oscillation tube.

Note that the type of residual force mentioned here is the difference of the total force from the force generated from the gradient of the potential. It is interesting to note that the extrema of the potential are not necessarily the same as the zeros of the drift force (46). From our view, this shift of zeroes is due to the presence of the residual force from the curl flux. We pointed out in this article that it might be possible to experimentally probe and quantify the curl flux force (the other critical component for describing nonequilibrium systems in addition to the potential or probability distribution) from the difference of the potential extrema from the probability distribution of the observables and zeroes of the drift force from the average of the observables.

SUPPORTING MATERIAL

Five figures and one table are available at http://www.biophysj.org/biophysj/supplemental/S0006-3495(09)01468-4.

We have used VCELL software (http://vcell.org) for part of our calculations in solving the diffusion equation. A minor error in implementing the models in VCELL is corrected here without significant changes of the previous results (29,50).

J.W. thanks the National Science Foundation (Career Award) and the American Chemical Society Petroleum Fund. L.X. and E.W. are supported by the National Natural Science Foundation of China (grant Nos. 90713022 and 20735003).

REFERENCES

1. McAdams, H. H., and A. Arkin. 1997. Stochastic mechanisms in gene expression. *Proc. Natl. Acad. Sci. USA*. 94:814–819.
2. Elowitz, M. B., and S. Leibler. 2000. A synthetic oscillatory network of transcriptional regulators. *Nature*. 403:335–338.
3. Swain, P. S., M. B. Elowitz, and E. D. Siggia. 2002. Intrinsic and extrinsic contributions to stochasticity in gene expression. *Proc. Natl. Acad. Sci. USA*. 99:12795–12800.
4. Thattai, M., and A. van Oudenaarden. 2001. Intrinsic noise in gene regulatory networks. *Proc. Natl. Acad. Sci. USA*. 98:8614–8619.
5. Vilar, J. M. G., C. C. Guet, and S. Leibler. 2003. Modeling network dynamics: the Lac operon, a case study. *J. Cell Biol.* 161:471–476.
6. Paulsson, J. 2004. Summing up the noise in gene networks. *Nature*. 427:415–418.

7. Hasty, J., J. Pradines, M. Dolnik, and J. J. Collins. 2000. Noise-based switches and amplifiers for gene expression. *Proc. Natl. Acad. Sci. USA*. 97:2075–2080.
8. Hasty, J., F. Isaacs, M. Dolnik, D. McMillen, and J. J. Collins. 2001. Designer gene networks: towards fundamental cellular control. *Chaos*. 11:207–220.
9. Harmer, S. L., S. Panda, and S. A. Kay. 2001. Molecular bases of circadian rhythms. *Annu. Rev. Cell Dev. Biol.* 17:215–253.
10. Fall, C. P., E. S. Marland, J. M. Wagner, and J. J. Tyson. 2002. Computational Cell Biology. Springer Verlag, New York.
11. Gonze, D., J. Halloy, and P. Gaspard. 2002. Biochemical clocks and molecular noise: theoretical study of robustness factors. *J. Chem. Phys.* 116:10997–11010.
12. Gonze, D., J. Halloy, and A. Goldbeter. 2002. Robustness of circadian rhythms with respect to molecular noise. *Proc. Natl. Acad. Sci. USA*. 99:673–678.
13. Tomita, J., M. Nakajima, T. Kondo, and H. Iwasaki. 2005. No transcription-translation feedback in circadian rhythm of KaiC phosphorylation. *Science*. 307:251–254.
14. Nakajima, M., K. Imai, H. Ito, T. Nishiwaki, Y. Murayama, et al. 2005. Reconstitution of circadian oscillation of cyanobacterial KaiC phosphorylation in vitro. *Science*. 308:414–415.
15. Nishiwaki, T., H. Iwasaki, M. Ishiura, and T. Kondo. 2000. Nucleotide binding and autophosphorylation of the clock protein KaiC as a circadian timing process of cyanobacteria. *Proc. Natl. Acad. Sci. USA*. 97:495–499.
16. Nishiwaki, T., Y. Satomi, M. Nakajima, C. Lee, R. Kiyohara, et al. 2004. Role of KaiC phosphorylation in the circadian clock system of *Synechococcus elongatus* PCC 7942. *Proc. Natl. Acad. Sci. USA*. 101:13927–13932.
17. Nishiwaki, T., Y. Satomi, Y. Kitayama, K. Terauchi, R. Kiyohara, et al. 2007. A sequential program of dual phosphorylation of KaiC as a basis for circadian rhythm in cyanobacteria. *EMBO J*. 26:4029–4037.
18. Rust, M. J., J. S. Markson, W. S. Lane, D. S. Fisher, and E. K. O'Shea. 2007. Ordered phosphorylation governs oscillation of a three-protein circadian clock. *Science*. 318:809–812.
19. Sasai, M., and P. G. Wolynes. 2003. Stochastic gene expression as a many-body problem. *Proc. Natl. Acad. Sci. USA*. 100:2374–2379.
20. Ao, P. 2004. Potential in stochastic differential equations: novel construction. *J. Phys. Math. Gen*. 37:L25–L30.
21. Zhu, X. M., L. Yin, L. Hood, and P. Ao. 2004. Calculating biological behaviors of epigenetic states in the phage-λ life cycle. *Funct. Integr. Genomics*. 4:188–195.
22. Qian, H., and D. A. Bear. 2005. Thermodynamics of stoichiometric biochemical networks far from equilibrium. *Biophys. Chem*. 114: 213–220.
23. Qian, H., and T. C. Reluga. 2005. Nonequilibrium thermodynamics and nonlinear kinetics in a cellular signaling switch. *Phys. Rev. Lett.* 94:028101.
24. Wang, J., B. Huang, X. F. Xia, and Z. R. Sun. 2006. Funneled landscape leads to robustness of cellular networks: MAPK signal transduction. *Biophys. J. Lett*. 91:L54–L56.
25. Wang, J., B. Huang, X. F. Xia, and Z. R. Sun. 2006. Funneled landscape leads to robustness of cell networks: yeast cell cycle. *PLOS Comp. Biol.* 2:e147.
26. Han, B., and J. Wang. 2007. Quantifying robustness of cell cycle network: funneled energy landscape perspectives. *Biophys. J*. 92: 3755–3763.
27. Kim, K. Y., and J. Wang. 2007. Potential energy landscape and robustness of a gene regulatory network: toggle switch. *PLOS Comput. Biol.* 33:e60.
28. Lapidus, S., B. Han, and J. Wang. 2008. Intrinsic noise, dissipation cost, and robustness of cellular networks: the underlying energy landscape of MAPK signal transduction. *Proc. Natl. Acad. Sci. USA*. 105: 6039–6044.
29. Wang, J., L. Xu, and E. K. Wang. 2008. Potential landscape and flux framework of non-equilibrium networks: robustness, dissipation and coherence of biochemical oscillations. *Proc. Natl. Acad. Sci. USA*. 105:12271–12276.
30. Wolynes, P. G., J. N. Onuchic, and D. Thirumalai. 1995. Navigating the folding routes. *Science*. 267:1619–1622.
31. Gardiner, C. W. 1985. Handbook of Stochastic Methods for Physics, Chemistry and the Natural Sciences. Springer-Verlag, Berlin, Germany.
32. van Kampen, N. G. 1992. Stochastic Processes in Chemistry and Physics. North-Holland, Amsterdam, The Netherlands.
33. Gillespie, D. T. 1977. Exact stochastic simulation of coupled chemical reactions. *J. Phys. Chem.* 81:2340–2361.
34. Arkin, A., J. Ross, and H. H. McAdams. 1998. Stochastic kinetic analysis of developmental pathway bifurcation in phage k-infected Escherichia coli cells. *Genetics*. 149:1633–1649.
35. Kepler, T. B., and T. C. Elston. 2001. Stochasticity in transcriptional regulation: origins, consequences, and mathematical representations. *Biophys. J*. 81:3116–3136.
36. Qian, H., S. Saffarian, and E. L. Elson. 2002. Concentration fluctuations in a mesoscopic oscillating chemical reaction system. *Proc. Natl. Acad. Sci. USA*. 99:10376–10381.
37. Bialek, W. 2003. Stability and noise in biochemical switches. *Adv. Neural Inform. Process.* 13:103–109.
38. Walczak, A. M., M. Sasai, and P. G. Wolynes. 2005. Self-consistent proteomic field theory of stochastic gene switches. *Biophys. J*. 88: 828–850.
39. Fisher, R. A. 1930. The Genetical Theory of Natural Selection. Clarendon, Oxford, UK.
40. Wright, S. 1932. The roles of mutation, inbreeding, crossbreeding and selection in evolution. *Proc. 6th Int. Congr. Gen*. 1:356–366.
41. Delbruck, M. 1949. Discussion. *In* Biological Units Endowed with Genetic Continuity, International Colloquium of the National Center for Scientific Research [Unites Biologiques Douees de Continuite Genetique Colloques, Internationaux du Centre National de la Recherche Scientifique]. CNRS, Paris, France.
42. Waddington, C. H. 1957. Strategy of the Gene. Allen and Unwin, London, UK.
43. Frauenfelder, H., S. G. Sligar, and P. G. Wolynes. 1991. The energy landscapes and motions of proteins. *Science*. 254:1598–1603.
44. Wang, J., and G. Verkhivker. 2003. Energy landscape theory, funnels, specificity and optimal criterion of biomolecular binding. *Phys. Rev. Lett*. 90:1–4.
45. Kageyama, H., T. Kondo, and H. Iwasaki. 2003. Circadian formation of clock protein complexes by KaiA, KaiB, KaiC, and SasA in cyanobacteria. *J. Biol. Chem*. 278:2388–2395.
46. Yin, L., and P. Ao. 2006. Existence and construction of dynamical potential in nonequilibrium processes without detailed balance. *J. Phys. Math. Gen*. 39:8593–8601.
47. Qian, H. 2001. Mesoscopic nonequilibrium thermodynamics of single macromolecules and dynamic entropy-energy compensation. *Phy. Rev. E*. 65:0161021–0161025.
48. Yoda, M., T. Ushikubo, W. Inoue, and M. Sasai. 2007. Roles of noise in single and coupled multiple genetic oscillators. *J. Chem. Phys*. 126: 1–11.
49. Zhu, X. M., L. Yin, and P. Ao. 2006. Limit cycle dynamics and conserved dynamics. *Int. J. Mod. Phys. B*. 20:817–827.
50. Wang, J., L. Xu, and E. K. Wang. 2008. Robustness, dissipations and coherence of the oscillation of circadian clock: potential landscape and flux perspectives. *PMC Biophys*. Published online 2008 December 30. Doi: 10.1186/1757-5036-1-7.